

# DOUBLE ASTEROID REDIRECTION TEST - MISSION DESIGN AND NAVIGATION

Justin A. Atchison<sup>(1)</sup>, Mark A. Jensenius<sup>(2)</sup>, Michelle H. Chen<sup>(2)</sup>,  
Nishant L. Mehta<sup>(2)</sup>, Christopher P. Dong<sup>(2)</sup>, and Andy Cheng<sup>(2)</sup>

<sup>(1)</sup>Johns Hopkins University Applied Physics Laboratory, 11100 Johns Hopkins Rd. Laurel, Maryland, 20723, (240) 228-1488, Justin.Atchison@jhuapl.edu

<sup>(2)</sup>Johns Hopkins University Applied Physics Laboratory, 11100 Johns Hopkins Rd. Laurel, Maryland, 20723, USA

**Abstract:** *The Double Asteroid Redirection Test (DART) will be the first space experiment to demonstrate asteroid impact hazard mitigation by using a kinetic impactor to deflect an asteroid. DART is the interceptor element of the Asteroid Impact & Deflection Assessment mission (AIDA), a joint NASA-ESA mission which also includes the ESA Asteroid Impact Monitor rendezvous mission. The primary goal of AIDA is to measure and characterize deflection of an asteroid by a kinetic impactor. The results will have implications for planetary defense, human spaceflight, and Near-Earth Object science and resource utilization. This paper describes the mission-design and navigation proposed to impact the secondary asteroid within the Didymos binary system. This analysis includes a simulation of closed-loop proportional navigation approach, which achieves the required precision targeting in spite of a very short detection timeline and many unknown target parameters.*

**Keywords:** *Asteroid Impact, Closed-Loop Navigation, Proportional Navigation, Binary Asteroid*

## 1 Introduction

Some 50-150 metric tons of cosmic material fall on the Earth every day, mainly in the form of dust, without causing harm to humanity. However, destructive impacts of large bodies on the Earth have occurred throughout geologic time and continue to the present. These are witnessed by the scars left on the surface of the Earth in the form of impact craters, over 150 of which have been identified. The largest of these are over 100 km in diameter. The occurrence of an impact large enough to create a 30 km crater would be a global disaster, and such impacts occur about once every million years. Even the impact of a small, 50 m asteroid, like the impact that caused the Tunguska Event of 1908, would have the potential to destroy a metropolitan area. Such impacts on Earth occur every few hundred years. An even smaller object, about 17 m in size, impacted over Chelyabinsk, Russia on Feb 15, 2013 and created an airburst that caused extensive damage and injured over 1,500 people.

The region of space close to the orbit of the Earth around the Sun is occupied by a population of small bodies known as Near-Earth Object (NEO)s. The impact hazard to Earth is dominated by

collisions with these NEOs. Over 95% of NEOs larger than 1 km in size have been discovered in ongoing asteroid searches, and fortunately none of these objects is likely to impact Earth. However, impacts of smaller objects, down to 140 m in size, would still cause significant disasters to Earth's population. As of early 2014, no more than a few percent of these hazardous objects are thought to have been discovered.

Discovering the hazardous NEOs is the necessary first step in responding to the NEO impact hazard. Dealing with this threat to humanity also requires mitigation methods. One response option is to attempt to deflect the hazardous object so that it does not impact the Earth. This paper considers the non-nuclear kinetic impactor technique, wherein a spacecraft impact is used to deflect an incoming asteroid. This technique has never been demonstrated and models vary with regards to how an incoming NEO might react to such an impact. The trajectory change resulting from a kinetic impact cannot be predicted accurately, because the response of an NEO to a hypervelocity spacecraft impact is highly uncertain. There are major gaps in our understanding of the nature of these bodies and of the physics of high speed collisions.

## **1.1 Mission Overview**

The Asteroid Impact & Deflection Assessment (AIDA) mission will be the first to demonstrate the kinetic impact technique and to measure the asteroid deflection. AIDA consists of two independent but mutually supporting mission concepts, one of which is the asteroid kinetic impactor and the other is the characterization and monitoring spacecraft. These two missions are, respectively, the Double Asteroid Redirection Test (DART) study, supported by National Aeronautics and Space Administration (NASA), and the Asteroid Impact Monitor (AIM) mission study supported by the European Space Agency (ESA).

DART is the kinetic impact spacecraft which will be targeted to intercept the secondary, or smaller, member of the binary asteroid Didymos in October, 2022. This approach has the advantage that the effects of the impact on the target's relative orbit are more observable than the effects on a heliocentric orbit. In this case, a relatively small spacecraft (~300 kg) can impart a measurable orbit change on the target. DART will include a coordinated ground-based observing and modeling campaign to study the asteroid deflection, which will produce a period change of the binary. AIM is a rendezvous mission which will monitor the results of the impact, measure precisely the amount of the asteroid deflection, and make critical measurements of the asteroids surface properties and interior structure so as to understand the response to the hypervelocity impact. Currently DART is a pre-Phase A study.

## 1.2 Mission Challenges

This experiment is intended to reveal unknown aspects of asteroid impact dynamics for planetary defense. To that end, the spacecraft's impact geometry and kinematics dictate mission requirements related to the approach conditions and targeting accuracy. In order to maximize the value of the impact, the spacecraft must hit the target near its center-of-mass. Doing so eliminates model uncertainties in the asteroid's mechanical responses to the impact. That is, a grazing impact is less relevant than a centrally placed impact. To this end, the encounter lighting conditions are critical to accurately determine the target location. Lighting conditions dictate the observability of the target and its companion, which affect both acquisition timing and targeting results. The ideal approach geometry would offer low solar phase angles.

It can be argued that the most observable change in the post-impacted asteroid's body is the secondary's binary orbit-period, which can be measured by AIM directly or from Earth using light-curve data. Orbit period change, equivalent to orbit energy change, is maximized when the spacecraft's approach velocity is parallel to the target's velocity at the time of impact. This geometry is achieved by finding an approach trajectory that lies in the plane of the binary system's moon and then by properly timing the impact. It's reasonable to assume that the arrival timing can be well controlled, such that the mission-design burden is to find an approach trajectory that lies nearly in the target's orbit plane. Then, the impact angle is defined as the angle between the target's primary-relative orbit plane and the spacecraft's arrival relative velocity. A trajectory that minimizes this angle produces a preferential change in the target's period.

By measuring the target's period about the primary member of the system, one can achieve a higher "signal" from a small impactor. That is, the heliocentric energy change from a small impact is quite challenging to measure. However, for the binary system, the small imparted energy will cause a relative period change sufficient to change the target's orbital phase by  $90^\circ$  over a period of months, an effect that is readily observable from light-curve data.

Finally, it is desirable for the spacecraft to arrive at the target when observers on the Earth can image the encounter using radar. This imposes an Earth-range constraint on the impact time and implies that the encounter must take place during defined windows when Didymos is near to its periape. This geometry is advantageous from a C3/delta-v perspective as well. Because this is a mission with international collaboration (mission partners as well as Earth-based observers), it is also desirable to have a single arrival date regardless of launch-date. This facilitates planning and cooperation across various partners.

## 1.3 Target Information

The target is Didymos (1996GT, 65803), a Near-Earth (Apollo) binary asteroid pair discovered in 1996 [1]. The system is an elliptical ( $e = 0.394$ ), inclined ( $3.407^\circ$  relative to ecliptic) orbit with

a period of 770.18 days. The primary asteroid rotates with a period of 2.2593 hr [1]. Scheirich and Pravec [2] studied light curve data spanning 29 days and computed the pair’s relative orbit geometry. The secondary orbits the primary with a period of 11.90 hr. The ratio of the secondary’s maximum dimension to the primary’s maximum dimension is 0.21. The pole of the orbit plane, given as right-ascension  $\lambda$  and declination  $\beta$  in the ecliptic plane is computed to be ( $\lambda = 157_{-7}^{+4}$ ,  $\beta = 19_{-15}^{+45}$ ) or ( $\lambda = 329_{-194}^{+11}$ ,  $\beta = -70_{-15}^{+25}$ ) degrees. The two solutions are quite different, and each has large uncertainties. With that in mind, the mission must accommodate large uncertainty in the system’s geometry, at least until additional observations are possible. This study uses the second solution, owing to the fact that it lies closer to the ecliptic. The secondary’s spin state is unknown. In a similar system, 1999KW4, the secondary is tidally locked [3], which is what is assumed for the Didymos secondary in this study. For this study, both asteroids are assumed to have a Bond albedo of 0.25. That, combined with the absolute magnitude of the system, corresponds to diameters of approximately 800 meters and 160 meters for the primary and secondary asteroids respectively.

#### 1.4 Spacecraft Capability

The spacecraft will be equipped with an Inertial Measurement Unit (IMU), a star-tracker, and 5 sun-sensors. This combination is intended to give  $< 15\mu\text{rad}$  ( $1\sigma$ ) and  $< 3\mu\text{rad/s}$  ( $1\sigma$ ) attitude estimation error. The attitude will be controlled using 12 thrusters and a dead-band strategy to maintain nominal pointing within acceptable limits.

In addition, the primary payload, the Long-Range Reconnaissance Imager (LORRI) serves as a sensor for locating, differentiating, and targeting the asteroid. LORRI, a narrow angle field-of-view Ritchey-Chretien telescope, is currently flying aboard the New Horizons mission to the Pluto system [4]. The LORRI design parameters are given in Table 1 below.

**Table 1: LORRI Parameters [4]**

Primary Mirror Diameter	20.8 cm
Focal Length	263 cm
Field-of-View	0.29°
Resolution	4.95 $\mu\text{rad/pixel}$
Array Size	1024 x 1024 pixel
Bandwidth	350-850 nm

## 2 Mission Design

Mission design is concerned with the trajectory design that satisfies the mission requirements and delivers sufficient approach hand-off conditions for the terminal guidance algorithms. Given that Didymos is a near-Earth target, direct chemical-propulsion trajectories were only considered. There are no deterministic  $\Delta V$  maneuvers; the launch vehicle provides the nominal impact trajectory.

### 2.1 Mission Phases

The mission is divided into four primary phases: Launch, Coast, Primary-Acquisition, and Terminal-Guidance.

The launch site will be Wallops Flight Facility (WFF) in Wallops, VA. In order to maintain simple launch operations, this analysis is only considering departure trajectories with declination of launch asymptote (DLA)s within +/- 38 degrees, corresponding to WFF's geocentric latitude. Launch trajectories with DLAs outside of these bounds would require a "dog-leg" launch or a parking orbit with an inclination change prior to departure from the Earth system [5, 6].

After launch, there are no required deterministic burns in the trajectory. This "coast" phase has Trajectory Correction Maneuvers (TCMs) only. Initial studies suggest that the launch dispersion corrections are the largest delta-v requirements. In addition, TCMs are employed to target the impact timing, which can vary by up to half the orbital period of Didymos's moon.

When the spacecraft is near enough to observe the Didymos primary, approximately 36 days prior to the impact event, the mission will transition to the "Primary Acquisition" phase. In this phase, optical navigation may be used to ensure that the spacecraft is on a correct trajectory to intercept the binary system.

Finally, when the spacecraft imager is able to differentiate the two members of the Didymos system and identify its target, the mission will transition to autonomous Terminal Guidance. This transition occurs approximately 1-3 hours prior to impact, owing to the small angular separation between the two members and the large variation in brightness. (The exact transition time depends on the imager's noise properties.) In this phase, the spacecraft will use proportional navigation to determine and command correction maneuvers, with limited to no human oversight.

## 2.2 Constraints

The trajectory design space is well characterized by “porkchop plots” that give relevant mission and arrival parameters over a grid of launch and arrival dates. The first available Earth/Didymos conjunction occurs in October 2022. This arrival date offers low-energy trajectories and the required close proximity for Earth radar imaging. Given that, porkchops plots were generated for that arrival date and departures dates starting as early as late 2019. These figures (Figures 1 - 3) are given below, with contours of launch energy (C3), DLA, solar phase angle, and impact angle. The first figure gives 2<sup>+</sup> year, 2<sup>+</sup> rev transfers, launching as early as 2019. The second figure gives 1<sup>+</sup> year, 1<sup>+</sup> rev transfers, launching in 2020. The final figure gives short arc (< 1 rev) transfers.

Departures are possible twice per year over the period of interest. Regions of the figures that are shaded red represent arrivals with poor solar phase angles (> 75°). Regions that are shaded green represent departures with DLAs outside of the bounds for a direct launch from WFF (< -38° or > 38°). The DLA constraint is relevant for this particular mission geometry because Didymos is inclined to Earth’s orbit, and is below (0.055 AU) the ecliptic at the time of Earth/Didymos close-approach. This inclination tends to drive the transfer  $\Delta V$ , since little energy is required to raise the orbit to the Didymos location (1.036 AU) at the time of conjunction.

## 2.3 Results

After the unfavorable regions are eliminated, there are four acceptable departure windows remaining. Selecting October 1 2022 as the fixed arrival date, a trajectory was selected for each region. These trajectories are summarized in Table 2 and illustrated in Figure 4 A-D. The Didymos/Earth line-of-nodes is illustrated. The arrival geometry places Didymos very near to Earth’s orbit, below the ecliptic. The transfer trajectory’s line-of-nodes is also illustrated. The favorable trajectories depart when these lines are approximately parallel, and the arrival location is perpendicular to the transfer trajectory’s line-of-nodes. Again, this geometry indicates that the inclination change is a driver for  $\Delta V$ . The arrival is “early” relative to the Earth/Didymos close-approach, owing to the arrival solar phase angle constraint. A solar phase angle < 75° requires the spacecraft to arrive with a velocity outbound relative to the sun. That is, the spacecraft must be between the sun and Didymos with a positive flight path angle prior to impact. This arrival is satisfied for earlier arrivals than the lowest energy arrival.

**Table 2: Trajectory Summaries**

	<b>Launch Date</b>	<b>C3 (<math>km^2/s^2</math>)</b>	<b>DLA (°)</b>	<b>Solar Phase (°)</b>	<b>Impact Angle (°)</b>
<b>A</b>	Jan 08 2020	3.68	35.6	57.5	30.6
<b>B</b>	Dec 20 2020	3.80	34.2	59.9	25.8
<b>C</b>	Dec 20 2021	3.74	35.0	59.8	25.7
<b>D</b>	Jun 17 2022	3.93	-37.4	42.6	26.6

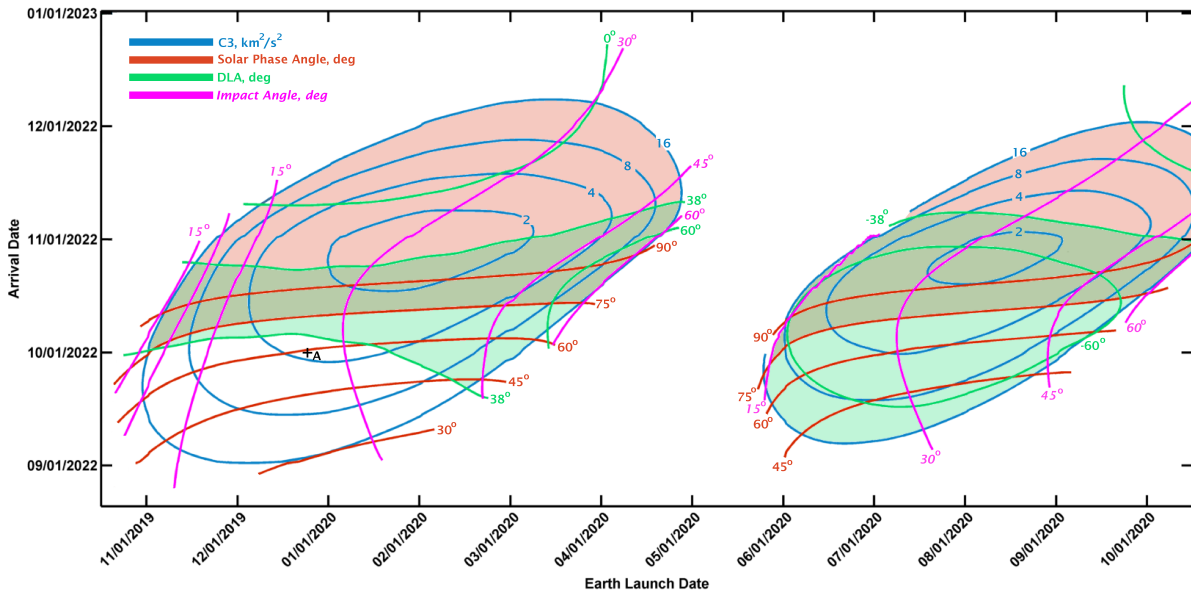


**Figure 1: Trajectory Options for 11/2019 to 11/2020 Launches**

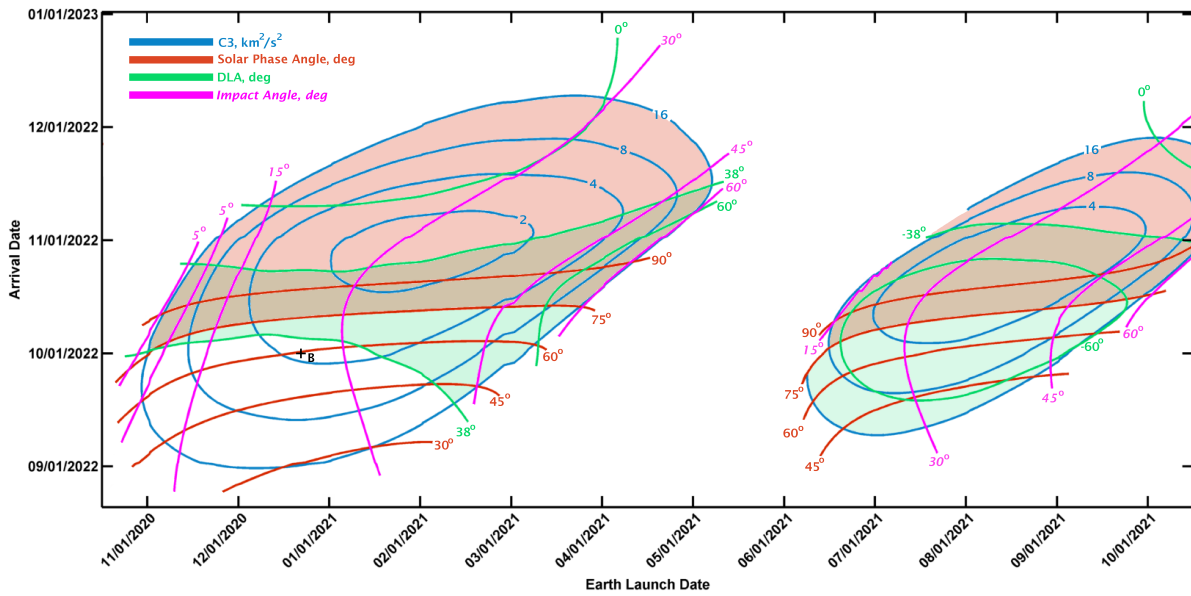


**Figure 2: Trajectory Options for 11/2020 to 11/2021 Launches**

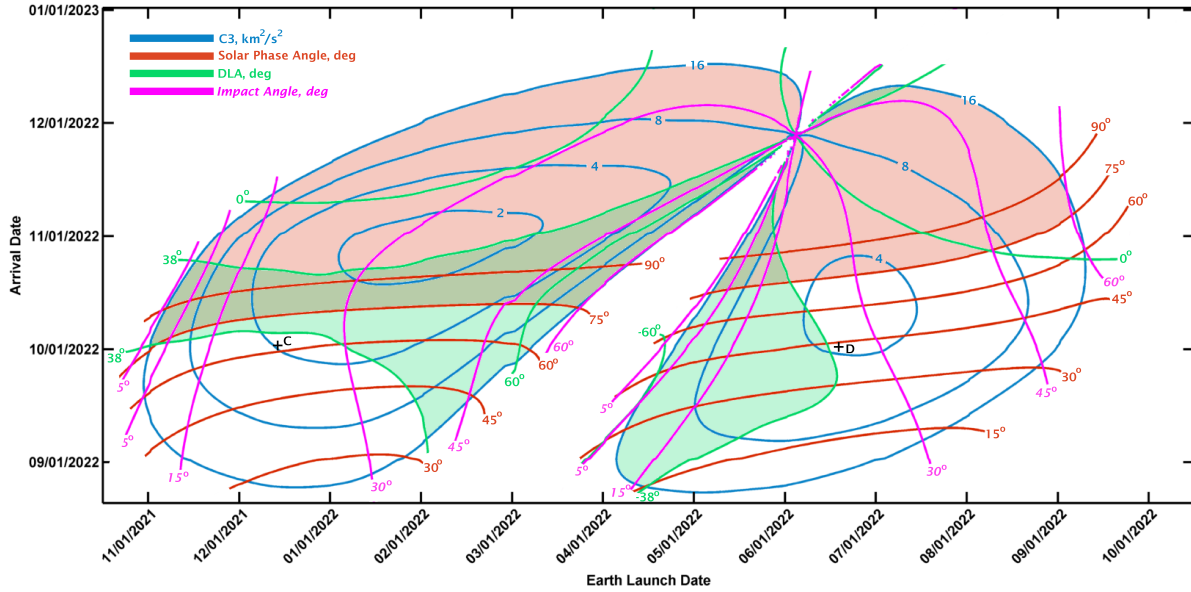


**Figure 3: Trajectory Options for 11/2021 to 11/2022 Launches**

Three of these direct transfers have opportunistic flybys of NEOs, as listed in Table 3. These encounters, if pursued, would offer additional science-return, as well as an opportunity to practice use of the acquisition and terminal-guidance navigation algorithms. In these cases, the thrust-commands would be disabled, such that the vehicle would compute a thrust command, but not deliver it to the spacecraft’s propulsion subsystem. The shortest trajectory (D) did not offer any flyby opportunities, though it’s not clear that there would be sufficient time in the short mission to incorporate one if identified. The asteroids are relatively small, based on their absolute magnitudes ( $H$ ). Two of them are classified as Potentially Hazardous Asteroids (PHA), so a short-range observation might prove additionally valuable to the planetary defense mission.

**Table 3: Sample Near-Earth Asteroid Flyby Opportunities**

	Date	Asteroid	$H$	Rel. Speed (km/s)	Earth Range (AU)
<b>A</b>	May 26 2021	2001 SX169 (PHA)	18.2	12.26	0.103
<b>B</b>	Mar 12 2021	2004 FX31	17.5	18.36	0.094
<b>C</b>	Jun 26 2022	1997 NC1 (PHA)	7.07	25.7	0.119

Finally, there is a possibility to consider resonant returns. In this approach, the DART trajectory would have a heliocentric period equal to half of Didymos’s heliocentric period (2:1). In the event of a missed impact, the spacecraft would complete two orbits before having a second impact opportunity. None of the previously identified trajectories satisfy this constraint. However, if a vehicle on one of them failed to intercept Didymos, a second opportunity (in Nov 2024) would require a burn on the order of 466 m/s. The costs and benefits of accommodating this additional  $\Delta V$  in the spacecraft design would have to be considered prior to launch.

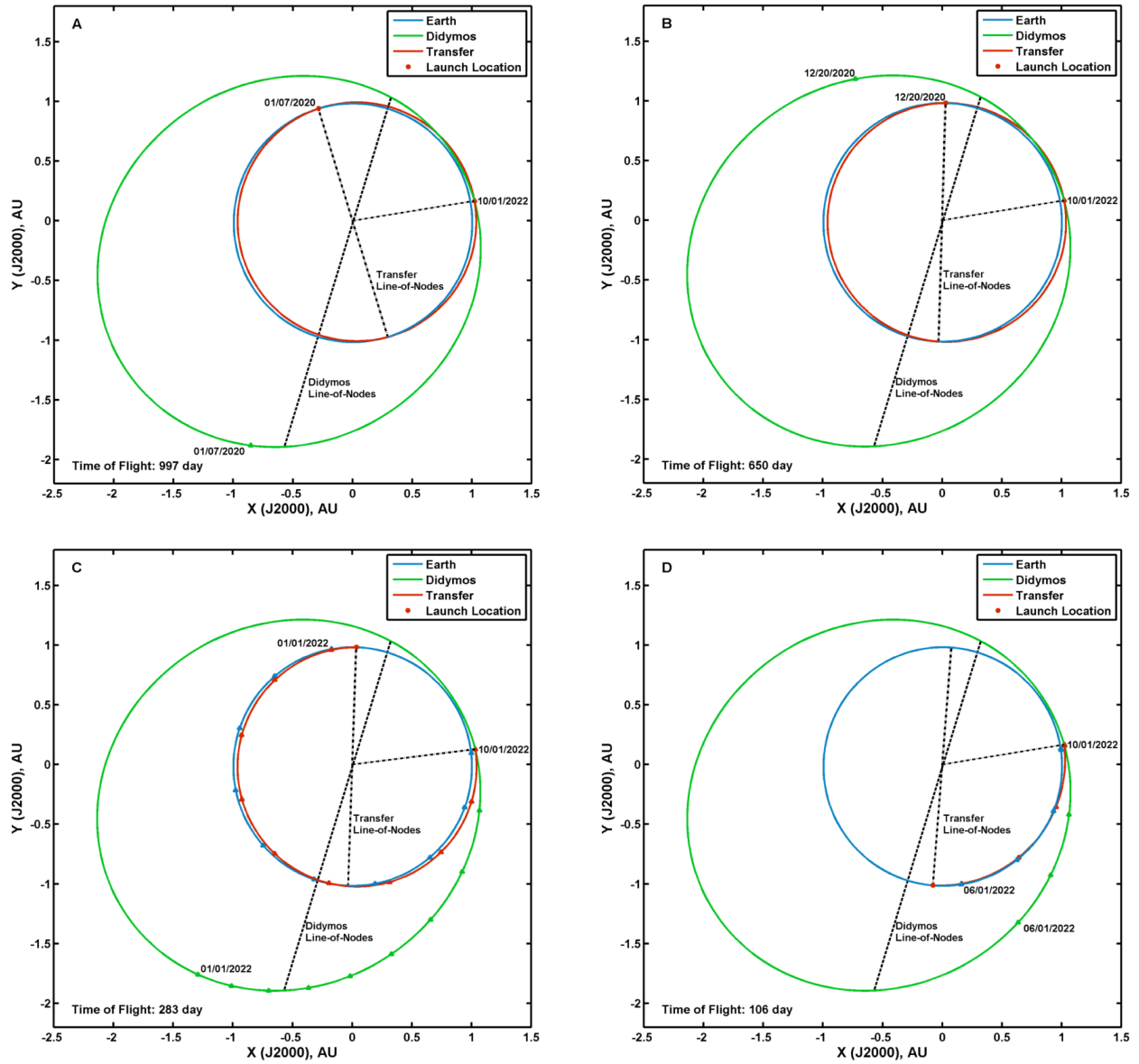


**Figure 4: Favorable Transfer Trajectories**

### 3 Navigation

The navigation component of the mission is concerned with achieving the designed trajectory and delivering the spacecraft to the target in satisfaction of the mission requirements.

#### 3.1 Launch and Coast Phases

During the *launch* and *coast* phases, the mission will use coherent radiometric Doppler and ranging as measurements to determine the spacecraft's position and velocity. TCMs will be commanded from the ground to compensate for launch-vehicle dispersions and apply corrections as the target's ephemeris is updated. The largest targeting TCM is associated with the impact timing. This maneuver must be conducted as early as possible, nominally at least 3-5 months before impact. In the case of the trajectories departing in 2022, the arrival/impact timing cannot be easily altered.

#### 3.2 Primary Acquisition

At approximately 36 days until impact, the Didymos primary system will be sufficiently observable for optical navigation. This marks the transition to the *primary acquisition* phase, in which spacecraft images from LORRI will be used to refine the ephemeris of the Didymos system.

Figure 5 shows a representative simulation of Didymos ephemeris improvement using space-based right-ascension and declination measurements from DART. The initial uncertainty is taken from the current published Didymos orbit knowledge<sup>1</sup>, which is taken to be representative of a typical tracking campaign. The measurement white noise is taken to be  $20 \mu\text{rad}$ , which is consistent with the spacecraft's expected attitude accuracy as well as a small margin for image processing errors. The angle biases are taken to be  $50 \mu\text{rad}$  ( $1\sigma$ ). The notional concept-of-operations is to command the spacecraft to take one hour of images at a 30 second cadence, twice per day. This approach manages the power and data-downlink requirements. The results are presented in radial, in-track, and cross-track directions defined relative to Didymos's heliocentric orbit. The uncertainty in Didymos's radial direction remains fairly constant, owing to its low observability near to the arrival time. That is, the spacecraft, Sun, and Didymos are nearly aligned. The final results give approximately 5 km uncertainty ( $1\sigma$  RSS) in the position of Didymos at 24 hours to impact. This roughly corresponds to a 0.5 second ( $1\sigma$ ) arrival time uncertainty and 4 km ( $1\sigma$ ) B-plane impact uncertainty.

---

<sup>1</sup>JPL Small Body Database, Solution Date: 2013-Aug-05 09:23:33

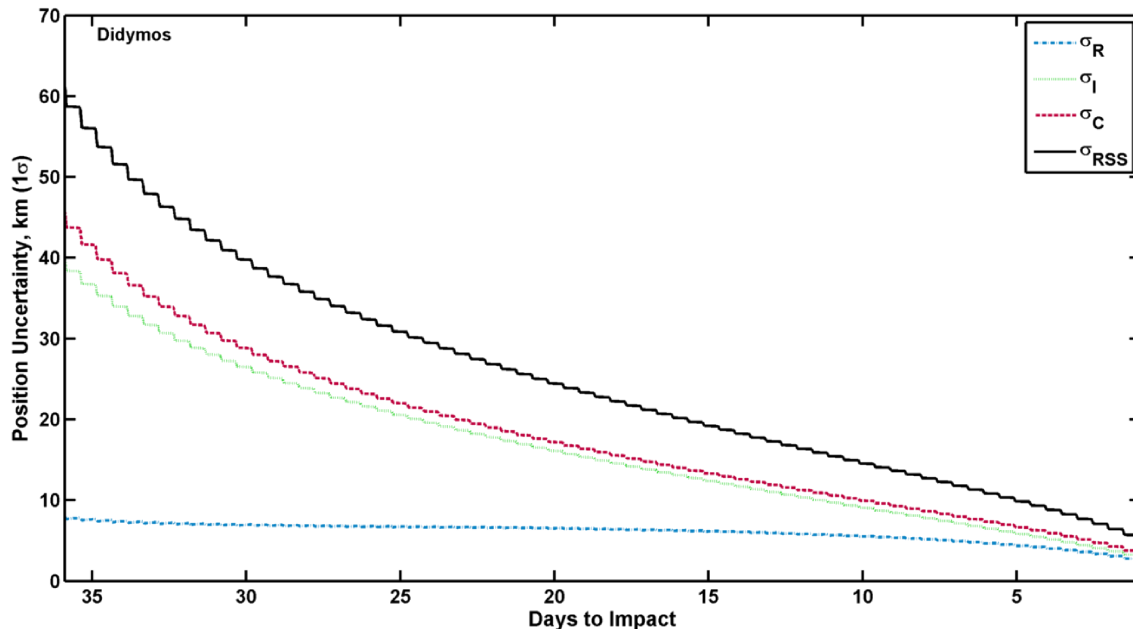


**Figure 5: Representative Didymos Ephemeris Refinement**

### 3.3 Terminal Guidance

At approximately 1-3 hours to impact, the navigation will be handed over to the spacecraft's autonomous *terminal guidance* mode. This transition occurs when the target is clearly distinguishable from the primary asteroid. The aim of the terminal guidance algorithms is to command thrusts that ensure the spacecraft impacts the target within specification, in the presence of many uncertainties.

In the past, a small-body collision was achieved using optical navigation for the Deep Impact mission, which impacted the comet Tempel 1 [7]. In that case, the target was 1000 times larger and the targeting precision was less stringent. As a result, the system was able to use three autonomously computed discrete maneuvers at predefined times [8]. Additional studies have considered how to extend this process to smaller targets[9]. In this case, the on-board autonomy is solving for the absolute orbit state of the target.

The approach considered in this paper uses a relative navigation algorithm derived from *proportional navigation*. Proportional navigation is a well-developed method familiar to the missile guidance community. Acceleration is commanded which is proportional to the line-of-site rate (often expressed as azimuth and elevation angles) between the interceptor and the target [10, 11, 12, 13]. The algorithm takes advantage of the basic fact that any two non-accelerating objects on an intercept course will have zero line-of-site rate in an inertial frame, regardless of range. Other studies have considered proportional navigation for the asteroid intercept problem and found favorable simulated performance [14, 15, 16, 17].

An advantage to proportional navigation is its robustness to uncertainty or small unmodeled accelerations. One source of this robustness is the assumption of linear relative motion between the asteroid and the spacecraft. The target asteroid's acceleration as it orbits about the primary is accounted for as process noise in the guidance filter. This approach removes the necessity of orbit determination and ensures convergence for a large range of measurements. Process noise also accounts for additional uncertainties, such as motion of the center-of-figure due to asteroid rotation. This robustness comes at the expense of  $\Delta V$  efficiency, insomuch as more complex approaches can better predict the future position of the target.

A initial study of the effectiveness of the terminal navigation algorithms is performed using a closed-loop simulation of the guidance filter and non-rotational spacecraft dynamics. The inputs were simulated using a truth-plus-noise model where the noise includes errors from the IMU, Star Tracker, Thrusters, and Centroiding algorithms.

The guidance filter was tuned using the expected noise levels. The simulation was run once with expected levels of noise and then again with significantly increased levels of noise. In the latter case, the guidance filter retains its original tuning. The fuel management and divert logic was implemented to control the number, timing, and duration of all thruster activity. This is in contrast with the typical mission profile that has thrust events scheduled at fixed times. By allowing the algorithm to make adjustments on-the-fly, the spacecraft becomes more robust to initial targeting errors or unexpected orbital dynamics.

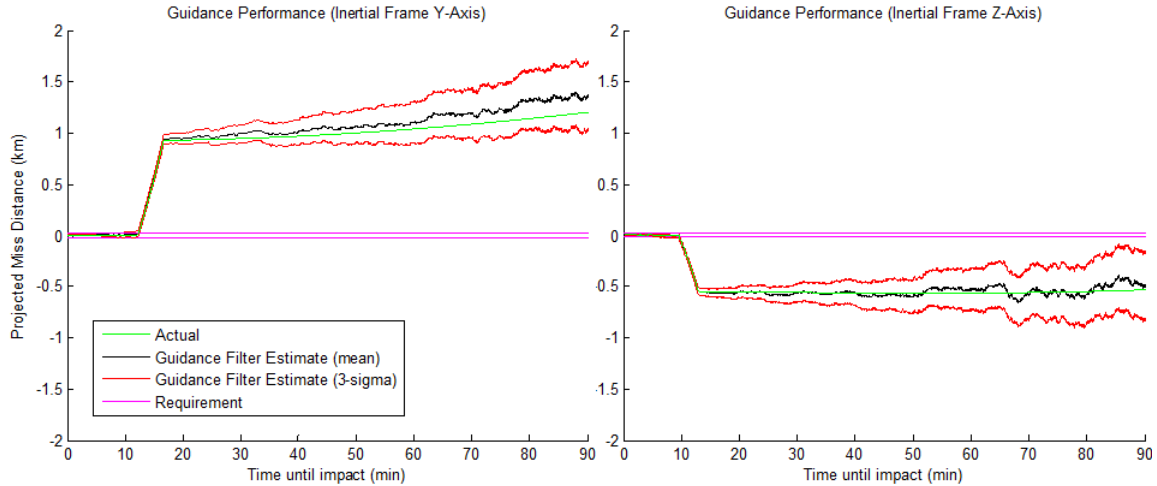
### **3.3.1 Guidance Results**

As mentioned previously, the closed-loop guidance simulation was run both in a nominal configuration (expected noise levels and initial targeting error) and in an off-nominal configuration (order-of-magnitude larger noise levels and initial targeting error). In the figures below, time progress from right to left with the impact occurring at time zero. The actual vehicle performance along with the filter estimates and uncertainty bounds are shown.

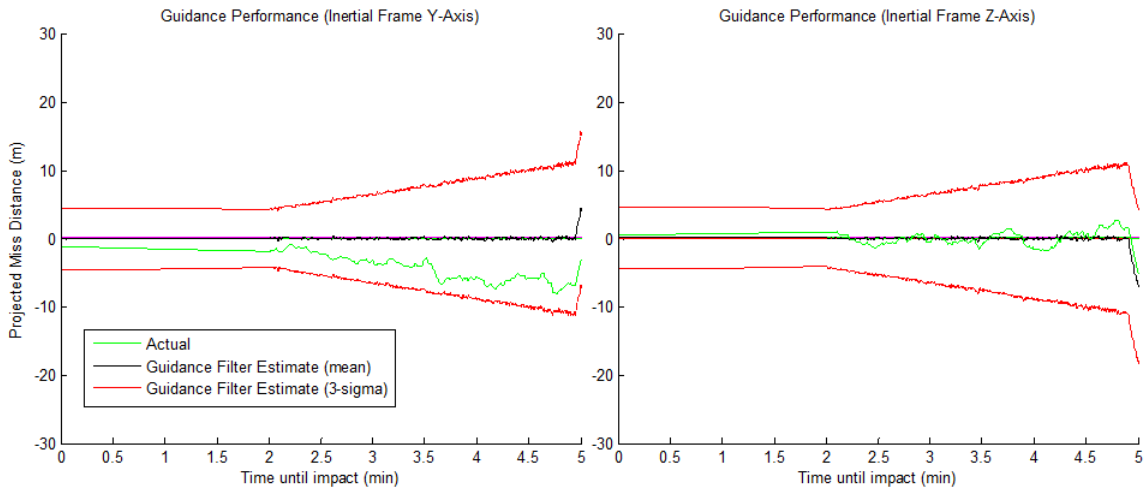
#### **Nominal Scenario**

Figure 6 shows performance during the full terminal guidance phase. The fuel management logic starts the first burn at approximately 16.5 minutes prior to impact and imparts a 1.9 m/s  $\Delta V$ .

Figure 7 shows the final five minutes prior to impact. This includes three minutes of continuous maneuvering and a final "quiet" period immediately prior to impact. Because the quality of measurement increases as range decreases, the three minutes of continuous maneuvering allows the spacecraft to make any final course corrections based on the most accurate measurements of the encounter. The continuous maneuvering phase uses an additional 0.5 m/s  $\Delta V$ .



**Figure 6: Filter and Vehicle Performance During Terminal Guidance**



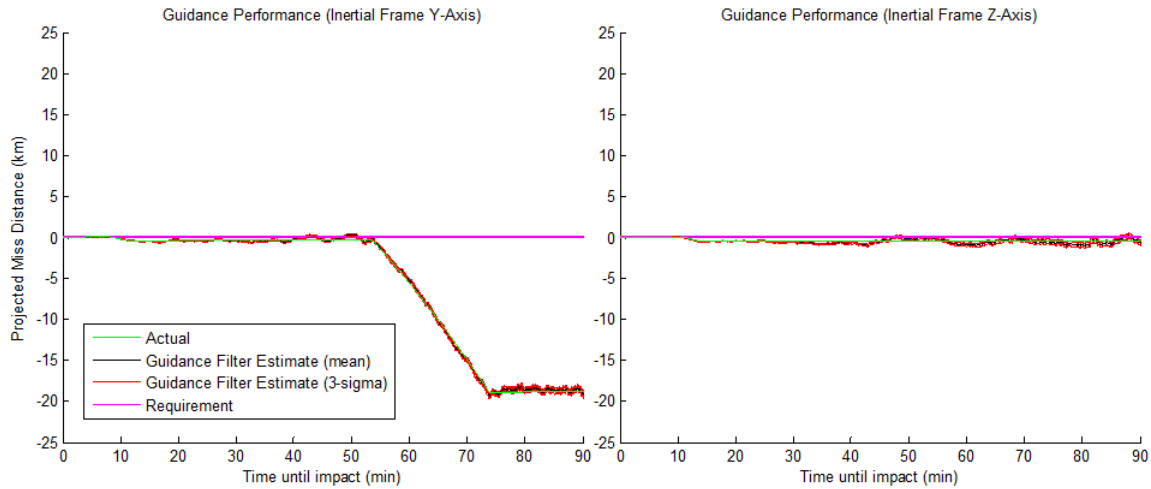
**Figure 7: Filter and Vehicle Performance During Final Five Minutes**

### Degraded Scenario

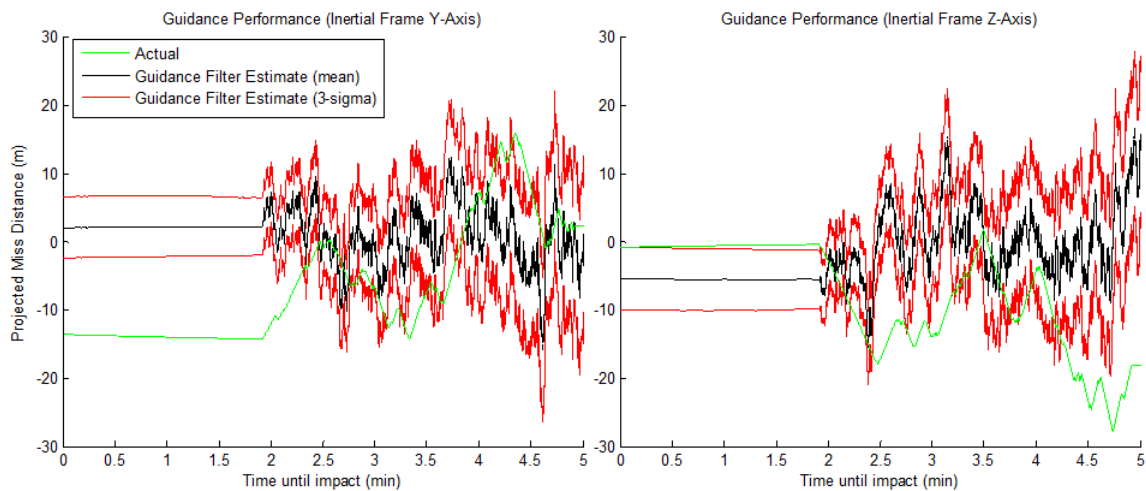
In this scenario, the spacecraft is given an initial targeting error of 20 km. Additionally, the IMU and centroiding noise is increased by a factor of 10. The guidance filter is not adjusted to reflect these new parameters, representing an unexpected degradation in system performance.

Figure 8 shows performance during the full terminal guidance phase. Due to the significantly larger initial targeting errors, the filter converges on a much larger projected miss distance and the logic starts the first burn at 74 minutes prior to impact, imparting a 4.9 m/s  $\Delta V$ . This is followed by a second burn at 14 minutes prior to impact, where a 1.5 meter-per-second  $\Delta V$  is commanded.

Figure 9 shows the final five minutes prior to impact. Again, this includes three minutes of continuous maneuvering and a final "quiet" period immediately prior to impact. The filter uncertainty bounds underestimate the error in the filter estimate, which is to be expected because the sensor noise levels are significantly higher than expected. The continuous maneuvering phase uses an additional 1.4 m/s  $\Delta V$ . The spacecraft is still able to impact the target, although the targeting performance is degraded.



**Figure 8: Filter and Vehicle Performance During Terminal Guidance**



**Figure 9: Filter and Vehicle Performance During Final Five Minutes**

## 4 Conclusion

The DART concept represents a step towards enabling asteroid mitigation via kinetic impact. The technologies and asteroid models that it matures are critical to our planet's defense. The Didymos system presents a reachable target in which one can conduct this meaningful experiment. The Didymos-Earth conjunction in October 2022 represents a readily achievable arrival date from a mission-design perspective. There are as many as four low-energy launch windows that arrive at the system on the same date while satisfying the mission's lighting and impact angle requirements. Once near to the asteroid, the on-board imager can produce sufficient measurements to enable autonomous impact guidance. Current simulations indicate that closed-loop proportional-navigation yields performance consistent with the required impact accuracies, in spite of the short target detection timeline.

## 5 Acknowledgments

The authors wish to thank Zachary Fletcher and Fazle Siddique of the Johns Hopkins University Applied Physics Laboratory for their important contributions to this effort.

## 6 Acronyms

**AIDA** Asteroid Impact & Deflection Assessment  
**AIM** Asteroid Impact Monitor  
**DART** Double Asteroid Redirection Test  
**DLA** declination of launch asymptote  
**ESA** European Space Agency  
**IMU** Inertial Measurement Unit  
**LORRI** Long-Range Reconnaissance Imager  
**NASA** National Aeronautics and Space Administration  
**NEO** Near-Earth Object  
**PHA** Potentially Hazardous Asteroids  
**TCMs** Trajectory Correction Maneuvers  
**WFF** Wallops Flight Facility

## 7 References

- [1] P. Pravec, L. A. M. Benner, M. C. Nolan, P. Kusnirak, D. Pray, J. D. Giorgini, R. F. Jurgens, S. J. Ostro, J.-L. Margot, C. Magri, A. Grauer, and S. Larson, “(65803) 1996 GT,” *Proceedings of the International Astronomical Union*, Vol. 8244, Nov. 2003, p. 2.
- [2] P. Scheirich and P. Pravec, “Modeling of lightcurves of binary asteroids,” *Icarus*, Vol. 200, October 2009, pp. 531–547.
- [3] S. J. Ostro, J.-L. Margot, L. A. Benner, J. D. Giorgini, D. J. Scheeres, E. G. Fahnestock, S. B. Broschart, J. Bellerose, M. C. Nolan, C. Magri, *et al.*, “Radar imaging of binary near-Earth asteroid (66391) 1999 KW4,” *Science*, Vol. 314, No. 5803, 2006, pp. 1276–1280.
- [4] A. F. Cheng, H. Weaver, S. Conrad, and e. al., “Long-Range Reconnaissance Imager on New Horizons,” *Space Science Reviews*, Vol. 140, October 2008, pp. 189–215.
- [5] V. C. C. Jr., “Design of Lunar and Interplanetary Ascent Trajectories,” *AIAA Journal*, Vol. 1, July 1963, pp. 1559–1567.
- [6] A. B. Sergeevsky, G. C. Snyder, and R. A. Cunniff, “Interplanetary Mission Design Handbook, Volume 1, Part 2,” *JPL Publication*, No. 43, 1982, pp. 1–34.
- [7] N. Mastrodemos, D. G. Kubitschek, and S. P. Synnott, “Autonomous Navigation for the Deep Impact Mission Encounter with Comet Tempel 1,” *Space Science Reviews*, Vol. 117, 2005, pp. 95–121.
- [8] D. G. Kubitschek, N. Mastrodemos, R. A. Werner, B. M. Kennedy, S. P. Synnott, G. W. Null, S. Bhaskaran, J. E. Riedel, and A. T. Vaughan, “Deep Impact Autonomous Navigation: the trials of targeting the unknown,” *29th Annual AAS Guidance and Control Conference, Breckenridge, Colorado, February 4-8, 2006.*, Pasadena, CA: Jet Propulsion Laboratory, National Aeronautics and Space Administration, 2006., 2006.
- [9] S. Bhaskaran and B. Kennedy, “Closed loop terminal guidance navigation for a kinetic impactor spacecraft,” *Acta Astronautica*, 2014, <http://dx.doi.org/10.1016/j.actaastro.2014.02.024>.
- [10] P. Zarchan, ed., *Tactical and Strategic Missile Guidance*, Vol. 199. Reston, VA: AIAA, fourth ed., 2002.
- [11] N. F. Palumbo, R. A. Blauwkamp, and J. M. Lloyd, “Basic Principles of Homing Guidance,” *Johns Hopkins APL Technical Digest*, Vol. 29, No. 1, 2010, pp. 25–41.
- [12] N. F. Palumbo, R. A. Blauwkamp, and J. M. Lloyd, “Modern Homing Missile Guidance

Theory and Techniques,” *Johns Hopkins APL Technical Digest*, Vol. 29, No. 1, 2010, pp. 42–59.

- [13] N. F. Palumbo, G. A. Harrison, R. A. Blauwkamp, and J. K. Marquart, “Guidance Filter Fundamentals,” *Johns Hopkins APL Technical Digest*, Vol. 29, No. 1, 2010, pp. 60–70.
- [14] M. Hawkins, A. Pitz, B. Wie, and J. Gil-Fernandez, “Terminal-Phase Guidance and Control Analysis of Asteroid Interceptors,” *AIAA Guidance, Navigation, and Control Conference*, Paper No. AIAA 2010-8348, 2-5 August 2010, Toronto, Ontario Canada.
- [15] M. Hawkins and B. Wie, “Impact-Angle Control of Asteroid Interceptors/Penetrators,” *21st AAS/AIAA Space Flight Mechanics Meeting*, Paper 2011-271, 2011, New Orleans LA.
- [16] Y. Guo, M. Hawkins, and B. Wie, “Optimal Feedback Guidance Algorithms for Planetary Landing and Asteroid Intercept,” *AAS/AIAA Astrodynamics Specialist Conference*, Paper 2011-588, 2011, Girdwood AK.
- [17] Y. Guo, M. Hawkins, and B. Wie, “Applications of Generalized Zero-Effort-Miss/Zero-Effort-Velocity Feedback Guidance Algorithm,” *Journal of Guidance, Control, and Dynamics*, Vol. 36, No. 3, 2013, pp. 810–820.